Integer Ambiguity Resolution with Tight and Soft Baseline Constraints for Freight Stabilization at Helicopters and Cranes

P. Jurkowski*, P. Henkel*, G. X. Gao** and C. Günther*,***
*Technische Universität München (TUM), Munich, Germany
**Stanford University, Stanford, USA
***German Aerospace Center (DLR), Oberpfaffenhofen, Germany

BIOGRAPHIES

Patryk Jurkowski is a master student in electrical engineering and information technology at the Technische Universität München, Germany. He recently finished his bachelor thesis on "Baseline constrained ambiguity resolution with multiple frequencies" with distinction. He also received the Bavarian regional prize in the European Satellite Navigation competition in 2010 for a differential carrier phase positioning system for freight stabilization at helicopters and cranes. Patryk worked as a student trainee on EGNOS performance and integrity - level B for Galileo at EADS Astrium from 2006 to 2010. He founded AMCONAV in 2011.

Patrick Henkel studied electrical engineering and information technology at the Technische Universität München, Munich, Germany, and the École Polytechnique de Montréal, Canada. He then started his PhD on reliable carrier phase positioning and recently graduated with "summa cum laude". He is now working towards his habilitation in the field of precise point positioning. He visited the Mathematical Geodesy and Positioning group at TU Delft as a guest researcher in 2007, and the GPS Lab at Stanford University in 2008 and 2010. Patrick received the Pierre Contensou Gold Medal at the International Astronautical Congress in 2007, and the Bavarian regional prize at the European Satellite Navigation Competition in 2010. He is one of the founders of AMCONAV.

Grace Xingxin Gao is a research associate at Stanford University. She received her B.S. in Mechanical Engineering in 2001 and her M.S. in Electrical Engineering in 2003, both from Tsinghua University, Beijing, China. She received the Ph.D. for her thesis entitled "Towards navigation based on 120 satellites: Analyzing the new signals" from Stanford University in 2008. She is also the recipient of the "2008 Young Achievement Award" from the Institute of Navigation. Her current research interests include Galileo signal and code structures, GNSS receiver architectures, and GPS modernization.

Christoph Günther studied theoretical physics at the Swiss Federal Institute of Technology in Zurich. He received his diploma in 1979 and completed his PhD in 1984. He worked on communication and information theory at Brown Boveri and Ascom Tech. From 1995, he led the development of mobile phones for GSM and later dual mode GSM/Satellite phones at Ascom. In 1999, he became head of the research department of Ericsson in Nuremberg. Since 2003, he is the director of the Institute of Communication and Navigation at the German Aerospace Center (DLR) and since December 2004, he additionally holds a Chair at the Technische Universität München (TUM). His research interests are in satellite navigation, communication and signal processing.

ABSTRACT

Carrier phase measurements are extremely accurate but ambiguous. The reliability of the resolution of this ambiguity is often not sufficient due to the the small carrier wavelength of 19 cm and multipath. There are two options for improving the reliability of integer least-squares estimation: (1) multi-frequency widelane combinations that increase the wavelength to several meters, and (2) constraints on the length and orientation of the baseline which reduce the size of the search space. This paper focuses on the second aspect, and provides a soft constrained integer least-squares estimator, i.e. a method that uses a priori information on the length and orientation of the baseline to improve the ambiguity resolution and also ensures a sufficient robustness with respect to uncertainties in the a priori information. This opens up new opportunities for applications such as freight stabilization on cranes and helicopters or attitude determination of aircrafts. In all these applications, the length and orientation are constrained but not fixed.

This paper suggests two approaches for soft constrained integer least-squares estimation: The first one includes a priori information on the length of the baseline and its orientation (attitude) in the form of Gaussian distributions.

The second one includes the a priori information by inequality constraints on the length and orientation. This information could come from physical constraints (e.g. gravity) or other sensors. Both approaches are solved iteratively with the Newton method.

The benefit of the a priori information depends on its variance or on the tightness of the inequality constraints. This paper shows that the new methods reduce the probability of wrong fixing with respect to unconstrained integer least-squares estimation by more than one order of magnitude even if the a priori information on the length is biased by 1 m. The proposed method is evaluated with both simulated and real measurements from PolaRx3G receivers of Septentrio.

INTRODUCTION

Differential carrier phase positioning is used in a wide range of applications including RTK services, assistance systems for cars, attitude determination of aircrafts, navigation of robots, and freight stabilization under helicopters.

Fig. 1 shows a helicopter that deposits beams near human workers. The pilot is not able to see the load, which results in dangerous situations for both the pilot and the ground staff. Using of two GNSS receivers (one onboard the helicopter and a second one on the carried freight) allows a determination of the relative position. It can then be used for stabilizing the freight by an assistance system.

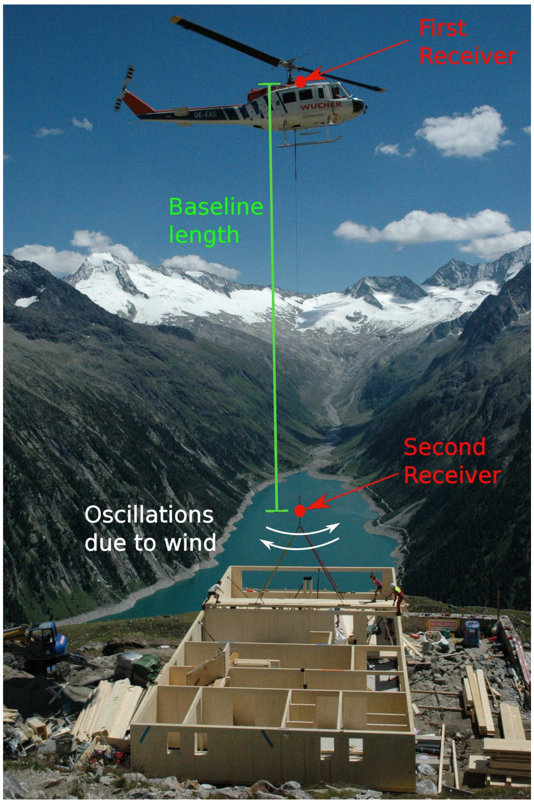

Fig. 1 Freight stabilization under helicopters: An a priori knowledge about the baseline length substantially improves the reliability of relative carrier phase positioning.

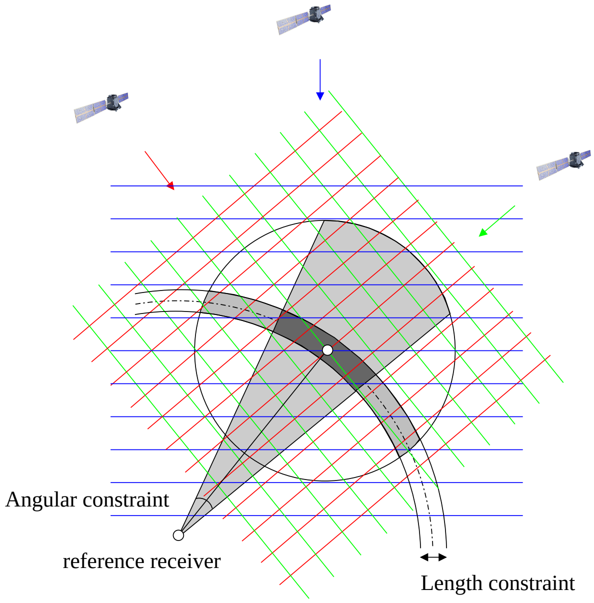

Fig. 2 Integer ambiguity grid: The search space volume of the float solution is substantially reduced by constraints on the baseline length and direction. As the length and direction are not perfectly known in many applications, a certain variation is allowed.

The use of carrier phase measurements allows millimeter accuracy but introduces integer ambiguities due to the periodicity of the phase. A reliable resolution of these integer ambiguities can be achieved by including a priori knowledge on the baseline into the ambiguity resolution: The length of the rope is essentially known (up to its extension due to the weight of the load), and its orientation is constrained by gravity and the energy accumulated in the maneuver.

Fig. 2 visualizes the constrained integer least-squares estimation for differential carrier phase positioning: The wavefronts from three satellites are shown, which intersect in the true receiver position. The pure code solution provides a rough estimate of the receiver position, which leads to a certain search space volume (shown as circle). The a priori knowledge on the length and orientation of the baseline further constrains the search space.

The Least-squares Ambiguity Decorrelation Adjustment (LAMBDA) method was developed by Teunissen in [1] to solve the unconstrained integer least-squares estimation. He introduced an integer ambiguity transformation based on an alternating sequence of permutations and integer decorrelations to obtain a sphere-like and largely decorrelated search space. Mönikes et al. introduced position domain constraints in the integer search in [2], and Teunissen provided a rigorous theory for integer least-squares estimation with a hard constraint on the baseline length in [3]. He extended his theory to a soft Gaussian constraint on the baseline length in [4]. However, he did not include any constraints on the baseline orientation. This is a non-trivial extension as the angles describing the baseline direction enter the cost function in a highly nonlinear form. However, soft constraints on the direction could be extremely helpful to reduce the size of the search space and, thereby, to improve the reliability of ambiguity resolution.

This paper proposes a maximum a posteriori probability estimator of the baseline length and direction with soft a priori information on both parameters. This estimator can be applied either to double difference measurements or to multi-frequency linear combinations of double differences. In [5]-[7], Henkel et al. proposed a class of multi-frequency code carrier linear combinations that maximize the ambiguity discrimination. It was introduced as the ratio between the wavelength and the doubled standard deviation of the combination noise to further improve the reliability of integer ambiguity resolution.

MEASUREMENT MODEL

The double difference carrier phase measurements on frequency f_m of satellite k are modeled in this paper by

$$\begin{aligned} \nabla\Delta\phi_m^k &= \nabla\Delta r^k + \lambda_m \nabla\Delta N_m^k \\ &\quad -q_{1m}^2 \nabla\Delta I^k + \Delta T^k + \nabla\Delta\eta_{\phi_m}^k, \end{aligned} \quad (1)$$

with the double difference range $\nabla\Delta r^k$, the double difference integer ambiguity $\nabla\Delta N_m^k$, the double difference ionospheric and tropospheric delays $\nabla\Delta I^k$ and $\nabla\Delta T^k$, the ratio of frequencies $q_{1m} = f_1/f_m$, and the double difference measurement noise $\nabla\Delta\eta_{\phi_m}^k$. Obviously, the double difference atmospheric delays can be neglected for short baselines as considered in the first part of this paper. A similar model is used for the double difference code measurements, i.e.

$$\nabla\Delta\rho_m^k = \nabla\Delta r^k + q_{1m}^2 \nabla\Delta I^k + \nabla\Delta T^k + \nabla\Delta\eta_{\rho_m}^k. \quad (2)$$

Two multi-frequency linear combinations are applied to the double difference carrier phase measurements $\lambda_m \nabla\Delta\boldsymbol{\phi}_m$ and code measurements $\nabla\Delta\boldsymbol{\rho}_m$: a code carrier linear combination and a code-only combination, i.e.

$$\boldsymbol{\Psi} = \begin{bmatrix} \sum_{m=1}^{M} (\alpha_m \lambda_m \nabla\Delta\boldsymbol{\phi}_m + \beta_m \nabla\Delta\boldsymbol{\rho}_m) \\ \sum_{m=1}^{M} (\beta'_m \nabla\Delta\boldsymbol{\rho}_m) \end{bmatrix}, \quad (3)$$

where α_m denote the weighting coefficients of the phase measurements, and β_m and β'_m represent the code coefficients on frequency $m \in \{1, \ldots, M\}$. These coefficients were optimized by Henkel et al. in [5]-[7]; the derivation is reviewed later in this paper. The combined measurements $\boldsymbol{\Psi}$ are modeled by

$$\boldsymbol{\Psi} = \boldsymbol{H}\boldsymbol{\xi} + \boldsymbol{A}\boldsymbol{N} + \boldsymbol{b} + \boldsymbol{\varepsilon}, \quad (4)$$

where $\boldsymbol{H}$ describes the differential geometry given by

$$\boldsymbol{H} = \begin{bmatrix} (\boldsymbol{e}^1)^T - (\boldsymbol{e}^K)^T \\ \vdots \\ (\boldsymbol{e}^{K-1})^T - (\boldsymbol{e}^K)^T \end{bmatrix}, \quad (5)$$

with the unit vector $\boldsymbol{e}^k$ pointing from the k-th satellite to the receiver, and $\boldsymbol{\xi}$ being the baseline between both receivers. It can be represented in spherical coordinates by the elevation ν_1, the azimuth ν_2 and the length l, i.e.

$$\boldsymbol{\xi} = \boldsymbol{r}(\nu_1, \nu_2) \cdot l, \quad (6)$$

with

$$\boldsymbol{r}(\nu_1, \nu_2) = \begin{bmatrix} \cos(\nu_1)\cos(\nu_2) \\ \cos(\nu_1)\sin(\nu_2) \\ \sin(\nu_1) \end{bmatrix}. \quad (7)$$

The second term in (4) represents the combined integer ambiguities $\boldsymbol{N}$ with the combination wavelength included in pre-factor matrix $\boldsymbol{A}$:

$$\boldsymbol{A} = \begin{bmatrix} \lambda \cdot \boldsymbol{I} \\ \boldsymbol{0} \end{bmatrix}. \quad (8)$$

The unknown biases $\boldsymbol{b}$ describe multipath with long decorrelation time, and are introduced to test the robustness of the constrained ambiguity resolution. The measurement noise $\boldsymbol{\varepsilon} \sim \mathcal{N}(\boldsymbol{0}, \boldsymbol{\Sigma})$ is assumed to be white Gaussian noise.

Unconstrained ambiguity resolution

The estimation of integer ambiguities and baselines is in general performed such that the weighted squared norm of range residuals is minimized. Teunissen decomposed this squared norm into three terms in [1]:

$$\begin{aligned} &\min_{\boldsymbol{\xi},\boldsymbol{N}} \|\boldsymbol{\Psi} - \boldsymbol{H}\boldsymbol{\xi} - \boldsymbol{A}\boldsymbol{N}\|^2_{\boldsymbol{\Sigma}^{-1}} \\ &\quad = \min_{\boldsymbol{N}} \left(\|\hat{\boldsymbol{N}} - \boldsymbol{N}\|^2_{\boldsymbol{\Sigma}^{-1}_{\hat{\boldsymbol{N}}}} + \min_{\boldsymbol{\xi}} \|\check{\boldsymbol{\xi}}(\boldsymbol{N}) - \boldsymbol{\xi}\|^2_{\boldsymbol{\Sigma}^{-1}_{\check{\boldsymbol{\xi}}(\boldsymbol{N})}} \right) \\ &\qquad + \|\boldsymbol{P}^{\perp}_{\bar{\boldsymbol{A}}} \boldsymbol{P}^{\perp}_{\boldsymbol{H}} \boldsymbol{\Psi}\|^2_{\boldsymbol{\Sigma}^{-1}}, \end{aligned} \quad (9)$$

where $\hat{\boldsymbol{N}}$ denotes the float ambiguity estimates, $\check{\boldsymbol{\xi}}(\boldsymbol{N})$ is the fixed baseline estimate, and $\boldsymbol{P}^{\perp}_{\boldsymbol{H}}, \boldsymbol{P}^{\perp}_{\bar{\boldsymbol{A}}}$ are orthogonal projections defined as

$$\begin{aligned} \boldsymbol{P}^{\perp}_{\boldsymbol{H}} &= \boldsymbol{1} - \boldsymbol{P}_{\boldsymbol{H}} = \boldsymbol{1} - \boldsymbol{H}\left(\boldsymbol{H}^T\boldsymbol{\Sigma}^{-1}\boldsymbol{H}\right)^{-1}\boldsymbol{H}^T\boldsymbol{\Sigma}^{-1} \\ \boldsymbol{P}^{\perp}_{\bar{\boldsymbol{A}}} &= \boldsymbol{1} - \boldsymbol{P}_{\bar{\boldsymbol{A}}} \\ &= \boldsymbol{1} - \bar{\boldsymbol{A}}\left(\bar{\boldsymbol{A}}^T\boldsymbol{\Sigma}^{-1}\bar{\boldsymbol{A}}\right)^{-1}\bar{\boldsymbol{A}}^T\boldsymbol{\Sigma}^{-1}, \end{aligned} \quad (10)$$

with

$$\bar{\boldsymbol{A}} = \boldsymbol{P}^{\perp}_{H}\boldsymbol{A}. \quad (11)$$

The float ambiguity estimates $\hat{\boldsymbol{N}}$ are given by

$$\begin{aligned} \hat{\boldsymbol{N}} &= \arg\min_{\boldsymbol{N}\in\mathbb{R}^{K\times 1}} \|\boldsymbol{P}^{\perp}_{\boldsymbol{H}}(\boldsymbol{\Psi} - \boldsymbol{A}\boldsymbol{N})\|^2_{\boldsymbol{\Sigma}^{-1}} \\ &= \left(\bar{\boldsymbol{A}}^T\boldsymbol{\Sigma}^{-1}\bar{\boldsymbol{A}}\right)^{-1}\bar{\boldsymbol{A}}^T\boldsymbol{\Sigma}^{-1}\boldsymbol{P}^{\perp}_{H}\boldsymbol{\Psi}, \end{aligned} \quad (12)$$

with covariance matrix $\boldsymbol{\Sigma}_{\hat{\boldsymbol{N}}} = \left(\bar{\boldsymbol{A}}^T \boldsymbol{\Sigma}^{-1} \bar{\boldsymbol{A}}\right)^{-1}$. Similarly, the fixed baseline solution $\check{\boldsymbol{\xi}}(\boldsymbol{N})$ is given by

$$\check{\boldsymbol{\xi}}(\boldsymbol{N}) = \min_{\boldsymbol{\xi} \in \mathbb{R}^{3\times 1}} \|\boldsymbol{\Psi} - \boldsymbol{H}\boldsymbol{\xi} - \boldsymbol{A}\boldsymbol{N}\|^2_{\boldsymbol{\Sigma}^{-1}}, \tag{13}$$

with the covariance matrix $\boldsymbol{\Sigma}_{\check{\boldsymbol{\xi}}(\boldsymbol{N})} = (\boldsymbol{H}^T \boldsymbol{\Sigma}^{-1} \boldsymbol{H})^{-1}$. For unconstrained ambiguity resolution, the second term in (9) can be made to zero by setting $\boldsymbol{\xi}$ to $\check{\boldsymbol{\xi}}(\boldsymbol{N})$. Consequently, optimal ambiguity resolution reduces to the minimization of the first term in (9). The last term describes the irreducible noise. The introduction of constraints on the length and/ or direction of the baseline prevents the setting $\boldsymbol{\xi} = \check{\boldsymbol{\xi}}(\boldsymbol{N})$ and, thus, a separate estimation of ambiguities and the baseline is no longer feasible.

INTEGER AMBIGUITY RESOLUTION WITH TIGHT AND SOFT CONSTRAINTS

The constrained ambiguity resolution is performed in four steps as shown in Fig. 3. First, an unconstrained float solution $\hat{\boldsymbol{N}}$ is determined from (12). Secondly, a search is performed which takes some a priori information about the baseline length ($\bar{l}$) and direction ($\bar{\nu}_1$, $\bar{\nu}_2$) into account, and results in a set of candidates $\{\check{\boldsymbol{N}}\}$. For each of these $\check{\boldsymbol{N}}$, the baseline parameters l, ν_1 and ν_2 are estimated iteratively with the Newton method. Finally, the integer vector $\boldsymbol{N}$ with minimum error norm is selected. The efficiency of the search can be further improved by applying an integer decorrelation to the float ambiguities similar to the unconstrained case [1].

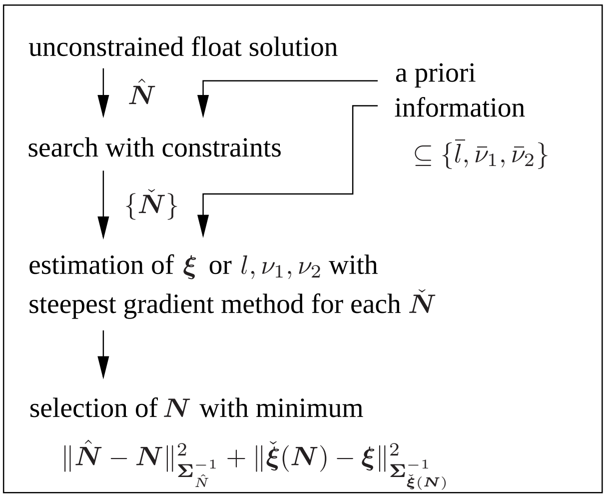

Fig. 3 Tight and soft constrained integer ambiguity resolution: A priori information is used for both the search and the baseline estimation.

The notation shall be simplified by denoting the second term in (9) by

$$J(\nu_1, \nu_2, l, \boldsymbol{N}) = \|\check{\boldsymbol{\xi}}(\boldsymbol{N}) - \boldsymbol{r}(\nu_1, \nu_2) l\|^2_{\boldsymbol{\Sigma}^{-1}_{\check{\boldsymbol{\xi}}(\boldsymbol{N})}}. \tag{14}$$

Tight constraints

The length of the baseline is known in a variety of applications, e.g. the distance between the freight and the helicopter in Fig. 1 is given by the length of the rope. This a priori knowledge can be considered either as a tight or as a soft constraint allowing some variations.

Length constraints

The minimization of J with a tight length constraint can be written as a Lagrange optimization, i.e.

$$f(\lambda, \boldsymbol{N}) = J(\nu_1, \nu_2, l, \boldsymbol{N}) + \lambda \cdot \left(\|\boldsymbol{\xi}\|^2 - l^2\right), \tag{15}$$

with Lagrange parameter λ. Setting the derivative with respect to $\boldsymbol{\xi}$ equal to zero, and solving it for $\boldsymbol{\xi}$ yields:

$$\check{\boldsymbol{\xi}}_\lambda(\boldsymbol{N}) = \left(\boldsymbol{\Sigma}^{-1}_{\check{\boldsymbol{\xi}}(\boldsymbol{N})} - \lambda \boldsymbol{I}\right)^{-1} \boldsymbol{\Sigma}^{-1}_{\check{\boldsymbol{\xi}}(\boldsymbol{N})} \check{\boldsymbol{\xi}}(\boldsymbol{N}), \tag{16}$$

which is set into the length constraint to obtain

$$g(\lambda) = \|\left(\boldsymbol{\Sigma}^{-1}_{\check{\boldsymbol{\xi}}(\boldsymbol{N})} - \lambda \boldsymbol{I}\right)^{-1} \boldsymbol{\Sigma}^{-1}_{\check{\boldsymbol{\xi}}(\boldsymbol{N})} \check{\boldsymbol{\xi}}(\boldsymbol{N})\|^2 - l^2 \overset{!}{=} 0. \tag{17}$$

It can be solved iteratively for λ with the Newton method, i.e.

$$\lambda_{n+1} = \lambda_n - \left.\frac{g(\lambda)}{g'(\lambda)}\right|_{\lambda=\lambda_n}, \tag{18}$$

with the gradient

$$g'(\lambda) = 2(\check{\boldsymbol{\xi}}(\boldsymbol{N}))^T \boldsymbol{\Sigma}^{-1}_{\check{\boldsymbol{\xi}}(\boldsymbol{N})} \left(\boldsymbol{\Sigma}^{-1}_{\check{\boldsymbol{\xi}}(\boldsymbol{N})} - \lambda \boldsymbol{I}\right)^{-3} \boldsymbol{\Sigma}^{-1}_{\check{\boldsymbol{\xi}}(\boldsymbol{N})} \check{\boldsymbol{\xi}}(\boldsymbol{N}). \tag{19}$$

The iterative computation can be initialized with $\lambda_0 = 0$, i.e. the unconstrained ambiguity resolution.

Angular constraints

In some applications, the direction of the baseline is known. Three cases shall be considered: the angle ν_1 is known only, the angle ν_2 is known only, and both angles are known a priori. If ν_1 is known, the minimization problem is given by

$$\min_{\nu_2, l, \boldsymbol{N}} \left(J(\nu_1, \nu_2, l, \boldsymbol{N})\right). \tag{20}$$

Setting the derivatives w.r.t. l and ν_2 to zero gives

$$\begin{aligned} \frac{\partial}{\partial l} \left(J(\nu_1, \nu_2, l, \boldsymbol{N})\right) = \\ - 2(\check{\boldsymbol{\xi}}(\boldsymbol{N}))^T \boldsymbol{\Sigma}^{-1}_{\check{\boldsymbol{\xi}}(\boldsymbol{N})} \boldsymbol{r}(\nu_1, \nu_2) \\ + 2l \cdot (\boldsymbol{r}(\nu_1, \nu_2))^T \boldsymbol{\Sigma}^{-1}_{\check{\boldsymbol{\xi}}(\boldsymbol{N})} \boldsymbol{r}(\nu_1, \nu_2) \overset{!}{=} 0, \end{aligned} \tag{21}$$

and

$$\frac{\partial}{\partial \nu_2}\left(J(\nu_1,\nu_2,l,\boldsymbol{N})\right) = -2l\cdot(\check{\boldsymbol{\xi}}(\boldsymbol{N}))^T\boldsymbol{\Sigma}^{-1}_{\check{\boldsymbol{\xi}}(\boldsymbol{N})}\frac{\partial \boldsymbol{r}(\nu_1,\nu_2)}{\partial \nu_2} + 2l^2\cdot\left(\frac{\partial \boldsymbol{r}(\nu_1,\nu_2)}{\partial \nu_2}\right)^T\boldsymbol{\Sigma}^{-1}_{\check{\boldsymbol{\xi}}(\boldsymbol{N})}\boldsymbol{r}(\nu_1,\nu_2) \stackrel{!}{=} 0. \quad (22)$$

As (21) and (22) can not be solved for l and ν_2 in closed form, an iterative solution based on the Newton method is suggested, i.e.

$$\check{l}^i(\boldsymbol{N}) = \check{l}^{i-1}(\boldsymbol{N}) - \left.\frac{\frac{\partial}{\partial l}\left(J(\nu_1,\nu_2,l,\boldsymbol{N})\right)}{\frac{\partial^2}{\partial^2 l}\left(J(\nu_1,\nu_2,l,\boldsymbol{N})\right)}\right|_{\substack{\nu_2=\check{\nu}_2^{i-1}(\boldsymbol{N})\\ l=\check{l}^{i-1}(\boldsymbol{N})}}, \quad (23)$$

and

$$\check{\nu}_2^i(\boldsymbol{N}) = \check{\nu}_2^{i-1}(\boldsymbol{N}) - \left.\frac{\frac{\partial}{\partial \nu_2}\left(J(\nu_1,\nu_2,l,\boldsymbol{N})\right)}{\frac{\partial^2}{\partial^2 \nu_2}\left(J(\nu_1,\nu_2,l,\boldsymbol{N})\right)}\right|_{\substack{\nu_2=\check{\nu}_2^{i-1}(\boldsymbol{N})\\ l=\check{l}^{i-1}(\boldsymbol{N})}}, \quad (24)$$

where the second order derivatives are given by

$$\frac{\partial^2}{\partial l^2}\left(J(\nu_1,\nu_2,l,\boldsymbol{N})\right) = 2(\boldsymbol{r}(\nu_1,\nu_2))^T\boldsymbol{\Sigma}^{-1}_{\check{\boldsymbol{\xi}}(\boldsymbol{N})}\boldsymbol{r}(\nu_1,\nu_2), \quad (25)$$

and

$$\frac{\partial^2}{\partial \nu_1^2}\left(J(\nu_1,\nu_2,l,\boldsymbol{N})\right) = -2l(\check{\boldsymbol{\xi}}(\boldsymbol{N}))^T\boldsymbol{\Sigma}^{-1}_{\check{\boldsymbol{\xi}}(\boldsymbol{N})}\frac{\partial^2 \boldsymbol{r}(\nu_1,\nu_2)}{\partial \nu_1^2} + 2l^2\left(\frac{\partial^2 \boldsymbol{r}(\nu_1,\nu_2)}{\partial \nu_1^2}\right)^T\boldsymbol{\Sigma}^{-1}_{\check{\boldsymbol{\xi}}(\boldsymbol{N})}\boldsymbol{r}(\nu_1,\nu_2) + 2l^2\left(\frac{\partial \boldsymbol{r}(\nu_1,\nu_2)}{\partial \nu_1}\right)^T\boldsymbol{\Sigma}^{-1}_{\check{\boldsymbol{\xi}}(\boldsymbol{N})}\frac{\partial \boldsymbol{r}(\nu_1,\nu_2)}{\partial \nu_1}, \quad (26)$$

where $\frac{\partial^2 \boldsymbol{r}(\nu_1,\nu_2)}{\partial \nu_1^2} = -\boldsymbol{r}(\nu_1,\nu_2)$.

If ν_2 is known instead of ν_1, the minimization problem is given by

$$\min_{\nu_1,l,\boldsymbol{N}}\left(J(\nu_1,\nu_2,l,\boldsymbol{N})\right), \quad (27)$$

which can be solved iteratively in a similar way. Setting the derivative w.r.t. ν_1 to zero gives

$$\frac{\partial}{\partial \nu_1}\left(J(\nu_1,\nu_2,l,\boldsymbol{N})\right) = -2l(\check{\boldsymbol{\xi}}(\boldsymbol{N}))^T\boldsymbol{\Sigma}^{-1}_{\check{\boldsymbol{\xi}}(\boldsymbol{N})}\frac{\partial \boldsymbol{r}(\nu_1,\nu_2)}{\partial \nu_1} + 2l^2\left(\frac{\partial \boldsymbol{r}(\nu_1,\nu_2)}{\partial \nu_1}\right)^T\boldsymbol{\Sigma}^{-1}_{\check{\boldsymbol{\xi}}(\boldsymbol{N})}\boldsymbol{r}(\nu_1,\nu_2) \stackrel{!}{=} 0. \quad (28)$$

The third case includes a tight a priori knowledge of both angles and, thus, removes the nonlinearity due to the trigonometric functions. The minimization problem turns into

$$\min_{l,\boldsymbol{N}} J(\nu_1,\nu_2,l,\boldsymbol{N}), \quad (29)$$

and can be solved in closed form for l, i.e.

$$\hat{l}(\boldsymbol{N}) = \frac{(\check{\boldsymbol{\xi}}(\boldsymbol{N}))^T\boldsymbol{\Sigma}^{-1}_{\check{\boldsymbol{\xi}}(\boldsymbol{N})}\boldsymbol{r}(\nu_1,\nu_2)}{(\boldsymbol{r}(\nu_1,\nu_2))^T\boldsymbol{\Sigma}^{-1}_{\check{\boldsymbol{\xi}}(\boldsymbol{N})}\boldsymbol{r}(\nu_1,\nu_2)}. \quad (30)$$

Soft constraints

The length and direction of the baseline are not perfectly known in many applications, e.g. the baseline between the freight and helicopter varies with elongation of the rope and oscillations due to wind and, thus, does not correspond to a vector in zenith direction of a priori known length. A similar situation occurs during attitude determination of aircrafts: In this case, the baseline length between two receivers on the wings varies due to bending. Therefore, soft constraints are introduced for both length and direction. These constraints can be either included in the form of a Gaussian distribution or a uniform distribution of the baseline length and direction.

Gaussian constraints

The constrained ambiguity resolution can be considered also as a maximum likelihood (ML) estimation or as a maximum a posteriori probability estimation. The latter one maximizes the a posteriori probability of the estimates of ν_1, ν_2 and l for a given set $\boldsymbol{\Psi}$. This maximization is rewritten with the rule of Bayes and the assumption of statistically independent ν_1, ν_2 and l as

$$\max_{\nu_1,\nu_2,l} p(\nu_1,\nu_2,l|\boldsymbol{\Psi}) = \max_{\nu_1,\nu_2,l} p(\boldsymbol{\Psi}|\nu_1,\nu_2,l)\cdot\frac{p(\nu_1)p(\nu_2)p(l)}{p(\boldsymbol{\Psi})}, \quad (31)$$

where the conditional probability is obtained from

$$p(\boldsymbol{\Psi}|\nu_1,\nu_2,l) = \frac{1}{\sqrt{(2\pi)^2|\boldsymbol{\Sigma}|}}e^{-\frac{1}{2}\|\boldsymbol{\Psi}-\boldsymbol{H}\boldsymbol{r}(\nu_1,\nu_2)l-\boldsymbol{A}\boldsymbol{N}\|^2_{\boldsymbol{\Sigma}^{-1}}} \quad (32)$$

and the a priori knowledge is assumed to be Gaussian distributed with known means and variances, i.e.

$$\begin{aligned} p(\nu_x) &= \frac{1}{\sqrt{2\pi\sigma^2_{\bar{\nu}_x}}}e^{-\frac{(\nu_x-\bar{\nu}_x)^2}{2\sigma^2_{\bar{\nu}_x}}}, \quad x\in\{1,2\} \\ p(l) &= \frac{1}{\sqrt{2\pi\sigma^2_{\bar{l}}}}e^{-\frac{(l-\bar{l})^2}{2\sigma^2_{\bar{l}}}}, \end{aligned} \quad (33)$$

and $p(\boldsymbol{\Psi})$ being a normalization given by

$$p(\boldsymbol{\Psi}) = \int p(\boldsymbol{\Psi}|\nu_1,\nu_2,l)p(\nu_1)p(\nu_2)p(l)d\nu_1 d\nu_2 dl. \quad (34)$$

The maximization of (31) can be simplified by taking the logarithm and omitting the pre-factor that does not depend on ν_1, ν_2 and l, i.e.

$$\begin{aligned}
&\min_{\nu_1,\nu_2,l,\boldsymbol{N}} \tilde{J}(\nu_1,\nu_2,l,\boldsymbol{N}) \\
&\quad = \min_{\nu_1,\nu_2,l,\boldsymbol{N}} \Big(\|\boldsymbol{\Psi} - \boldsymbol{H}\boldsymbol{r}(\nu_1,\nu_2)l - \boldsymbol{A}\boldsymbol{N}\|^2_{\boldsymbol{\Sigma}^{-1}} \\
&\qquad\quad + \frac{(l-\bar{l})^2}{\sigma^2_{\bar{l}}} + \frac{(\nu_1-\bar{\nu}_1)^2}{\sigma^2_{\bar{\nu}_1}} + \frac{(\nu_2-\bar{\nu}_2)^2}{\sigma^2_{\bar{\nu}_2}}\Big), \qquad (35)
\end{aligned}$$

which corresponds to the minimization of the first two terms of the unconstrained cost function of (9) plus three additive terms. The optimization over $\boldsymbol{N}$ is done in two steps: A search of a candidate set (that is described later) and a selection of the best candidate that minimizes the cost function $\tilde{J}$. For a fixed candidate $\boldsymbol{N}$, the optimization over l and ν_x, $x \in \{1,2\}$ is performed by setting the derivatives equal to zero:

$$\begin{aligned}
&\frac{\partial}{\partial l}\left(\tilde{J}(\nu_1,\nu_2,l,\boldsymbol{N})\right) = -2(\check{\boldsymbol{\xi}}(\boldsymbol{N}))^T \boldsymbol{\Sigma}^{-1}_{\check{\boldsymbol{\xi}}(\boldsymbol{N})} \boldsymbol{r}(\nu_1,\nu_2) \\
&\quad + 2l\cdot(\boldsymbol{r}(\nu_1,\nu_2))^T \boldsymbol{\Sigma}^{-1}_{\check{\boldsymbol{\xi}}(\boldsymbol{N})} \boldsymbol{r}(\nu_1,\nu_2) + \frac{2(l-\bar{l})}{\sigma^2_{\bar{l}}} \overset{!}{=} 0, \qquad (36)
\end{aligned}$$

and

$$\begin{aligned}
&\frac{\partial}{\partial \nu_x}\left(\tilde{J}(\nu_1,\nu_2,l,\boldsymbol{N})\right) = \\
&\quad -2l\cdot(\check{\boldsymbol{\xi}}(\boldsymbol{N}))^T \boldsymbol{\Sigma}^{-1}_{\check{\boldsymbol{\xi}}(\boldsymbol{N})} \frac{\partial \boldsymbol{r}(\nu_1,\nu_2)}{\partial \nu_x} \\
&\quad + 2l^2 \cdot \left(\frac{\partial \boldsymbol{r}(\nu_1,\nu_2)}{\partial \nu_x}\right)^T \boldsymbol{\Sigma}^{-1}_{\check{\boldsymbol{\xi}}(\boldsymbol{N})} \boldsymbol{r}(\nu_1,\nu_2) \\
&\quad + \frac{2(\nu_x-\bar{\nu}_x)}{\sigma^2_{\bar{\nu}_x}} \overset{!}{=} 0, \qquad (37)
\end{aligned}$$

which can be solved again iteratively with the Newton method.

Fig. 4 shows the benefit of tight and soft length constraints for integer least-squares estimation (ILS) [8]: The tight constraint (TC) reduces the probability of wrong unconstrained fixing by more than four orders of magnitude if the a priori length information is correct. The error rates are based on a simulation of Galileo double difference phase measurements on E1 and E5 of 4 epochs for a short baseline of 30 m. Phase-only measurements were considered to avoid code multipath, and a widelane combination with a wavelength of 78.1 cm was used to increase the success rate. A satellite geometry with 8 visible satellites was selected to obtain a typical performance. Obviously, the tight constraint makes the fixing also sensitive w.r.t. erroneous a priori information, i.e. it degrades the unconstrained performance if the error in the a priori information exceeds 50 cm. The soft constrained (SC) fixing takes the uncertainty in the length information into account and, thereby, improves the unconstrained fixing for any quality of the a priori information.

The reliability of ambiguity resolution can be further improved by including measurements from multiple epochs, i.e. by generalizing the cost function of (35) to

$$\begin{aligned}
\tilde{J} \;=\; &\sum_{i=1}^{I}\Big(\|\boldsymbol{\Psi}_i - \boldsymbol{H}_i\boldsymbol{r}_i l_i - \boldsymbol{A}\boldsymbol{N}\|^2_{\boldsymbol{\Sigma}^{-1}} \\
&+ \frac{(l_i-\bar{l}_i)^2}{\sigma^2_{\bar{l}_i}} + \frac{(\nu_{1,i}-\bar{\nu}_{1,i})^2}{\sigma^2_{\bar{\nu}_{1,i}}} + \frac{(\nu_{2,i}-\bar{\nu}_{2,i})^2}{\sigma^2_{\bar{\nu}_{2,i}}}\Big), \qquad (38)
\end{aligned}$$

which can be minimized over $\nu_{x,i}$ and l_i jointly with the iterative Newton method.

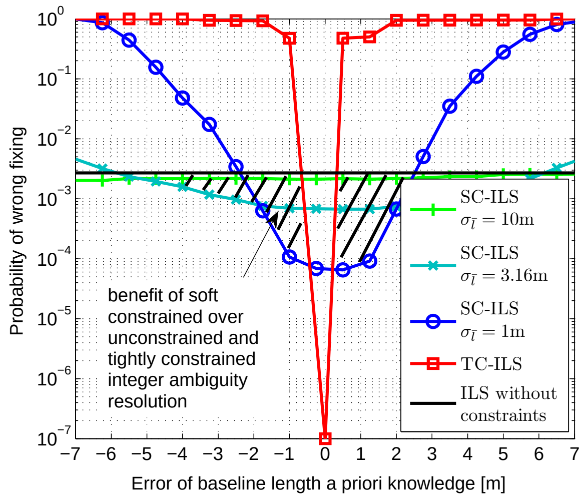

Fig. 4 Comparison of unconstrained, soft constrained and tightly constrained ambiguity resolution for erroneous baseline length a priori information: The tightly constrained ambiguity resolution outperforms the unconstrained and soft constrained fixing for perfect a priori knowledge but is extremely sensitive w.r.t. erroneous a priori information. The soft constrained ambiguity fixing benefits from the a priori information even if it is biased.

In the n-th step, the estimate of the baseline and ambiguity parameters is given by

$$\begin{bmatrix} \hat{\boldsymbol{\nu}}_1^{n+1} \\ \hat{\boldsymbol{\nu}}_2^{n+1} \\ \hat{\boldsymbol{l}}^{n+1} \\ \hat{\boldsymbol{N}}^{n+1} \end{bmatrix} = \begin{bmatrix} \hat{\boldsymbol{\nu}}_1^{n} \\ \hat{\boldsymbol{\nu}}_2^{n} \\ \hat{\boldsymbol{l}}^{n} \\ \hat{\boldsymbol{N}}^{n} \end{bmatrix} - \boldsymbol{S}^{-1} \begin{bmatrix} \frac{\partial \tilde{\boldsymbol{J}}}{\partial \boldsymbol{\nu}_1} \\ \frac{\partial \tilde{\boldsymbol{J}}}{\partial \boldsymbol{\nu}_2} \\ \frac{\partial \tilde{\boldsymbol{J}}}{\partial \boldsymbol{l}} \\ \frac{\partial \tilde{\boldsymbol{J}}}{\partial \boldsymbol{N}} \end{bmatrix}, \qquad (39)$$

where $\hat{\boldsymbol{\nu}}_x$, $x \in \{1,2\}$, and $\hat{\boldsymbol{l}}$ include the estimates of all epochs, and the Hesse matrix is given by

$$\boldsymbol{S} = \begin{bmatrix} \frac{\partial^2 \tilde{\boldsymbol{J}}}{\partial^2 \boldsymbol{\nu}_1} & \frac{\partial^2 \tilde{\boldsymbol{J}}}{\partial \boldsymbol{\nu}_1 \partial \boldsymbol{\nu}_2} & \frac{\partial^2 \tilde{\boldsymbol{J}}}{\partial \boldsymbol{\nu}_1 \partial \boldsymbol{l}} & \frac{\partial^2 \tilde{\boldsymbol{J}}}{\partial \boldsymbol{\nu}_1 \partial \boldsymbol{N}} \\ \frac{\partial^2 \tilde{\boldsymbol{J}}}{\partial \boldsymbol{\nu}_1 \partial \boldsymbol{\nu}_2} & \frac{\partial^2 \tilde{\boldsymbol{J}}}{\partial^2 \boldsymbol{\nu}_2} & \frac{\partial^2 \tilde{\boldsymbol{J}}}{\partial \boldsymbol{\nu}_2 \partial \boldsymbol{l}} & \frac{\partial^2 \tilde{\boldsymbol{J}}}{\partial \boldsymbol{\nu}_2 \partial \boldsymbol{N}} \\ \frac{\partial^2 \tilde{\boldsymbol{J}}}{\partial \boldsymbol{\nu}_1 \partial \boldsymbol{l}} & \frac{\partial^2 \tilde{\boldsymbol{J}}}{\partial \boldsymbol{\nu}_2 \partial \boldsymbol{l}} & \frac{\partial^2 \tilde{\boldsymbol{J}}}{\partial^2 \boldsymbol{l}} & \frac{\partial^2 \tilde{\boldsymbol{J}}}{\partial \boldsymbol{l} \partial \boldsymbol{N}} \\ \frac{\partial^2 \tilde{\boldsymbol{J}}}{\partial \boldsymbol{\nu}_1 \partial \boldsymbol{N}} & \frac{\partial^2 \tilde{\boldsymbol{J}}}{\partial \boldsymbol{\nu}_2 \partial \boldsymbol{N}} & \frac{\partial^2 \tilde{\boldsymbol{J}}}{\partial \boldsymbol{l} \partial \boldsymbol{N}} & \frac{\partial^2 \tilde{\boldsymbol{J}}}{\partial^2 \boldsymbol{N}} \end{bmatrix}. \qquad (40)$$

The iterative Newton method does not necessarily converge to the global optimum due to the nonlinearity of the cost function. One could perform the optimization for several random initializations around the a priori information and select the one with minimum $\tilde{J}$ to improve the probability of finding the global minimum. However, a single initialization was sufficient to find the global minimum in the following analysis.

Fig. 5 and 6 show the achievable accuracies for the soft constrained estimation of a vertical baseline with $l = 10$ m. The minimization of (38) ensures an optimal trade-off between the minimization of the weighted range residuals and the minimization of the weighted difference between the estimated baseline parameters and their a priori knowledge. Consequently, the achievable accuracies depend on the accuracy of the double difference measurements (or, more specifically, on the accuracy of the widelane phase-only combination with $\lambda = 78.1$ cm) and the accuracy of the a priori information ($\sigma_{\nu_1} = 30°$, $\sigma_{\nu_2} = \infty$, $\sigma_l = 10$cm). Obviously, the elevation of the baseline can be determined with a higher accuracy than the length due to the relatively long baseline.

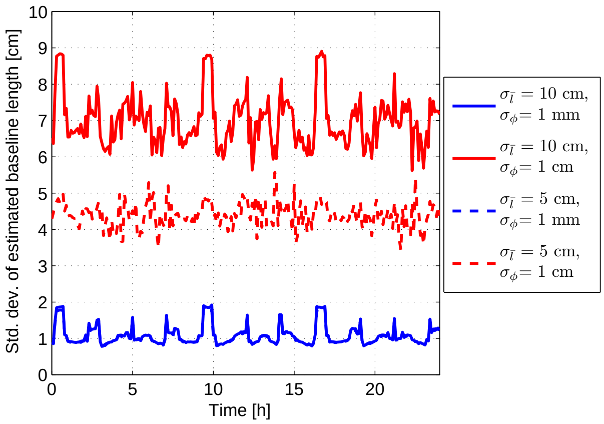

Fig. 5 Soft constrained estimation of baseline length for $l = 10$ m and $\nu_1 = 90°$: The achievable accuracy depends on the noise level of the measurements, the noise amplifications due to double differencing, widelane combinations and the geometry, and the quality of the a priori information. The latter one becomes especially beneficial for an increased phase noise level.

Constrained integer search

The integer ambiguities are determined by a tree search as shown in Fig. 7. The efficiency of the search can be substantially improved by some constraints on the length and direction of the baseline. The following notation shall be introduced for the tree search: The level in vertical direction is denoted by $k \in \{1, \ldots, K\}$ corresponding to the ambiguity indices, $j_k \in \{1, \ldots, c^k\}$ represents the path number

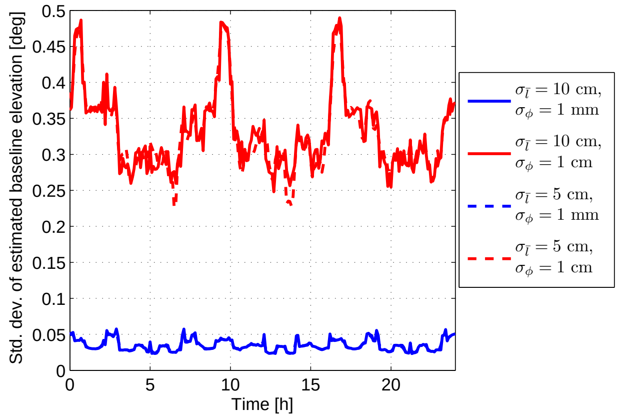

Fig. 6 Soft constrained estimation of baseline elevation for $l = 10$ m and $\nu_1 = 90°$: The a priori knowledge has only a minor impact on the estimation of the elevation due to the large baseline length, which enables a precise computation of its elevation.

at the k-th level, and c_k is the number of paths at the k-th level. The set of integer candidates at level k is denoted by $s^k = \{\check{N}_1^k, \ldots, \check{N}_{c_k}^k\}$.

The search aims on finding all integer vectors $\boldsymbol{N}$ that fulfill $\|\hat{\boldsymbol{N}} - \boldsymbol{N}\|^2_{\boldsymbol{\Sigma}^{-1}_{\hat{N}}} \leq \chi^2$, which can also be written in sequential form as

$$\begin{aligned} &|N^k - \hat{N}^k_{j_k|j_1,\ldots,j_{k-1}}| \\ &\leq \sigma_{\hat{N}_{k|1,\ldots,k-1}} \sqrt{\chi^2 - \sum_{l=1}^{k-1} \frac{\left(\check{N}^l_{j_l} - \hat{N}^l_{j_l|j_1,\ldots,j_{l-1}}\right)^2}{\sigma^2_{\hat{N}_{l|1,\ldots,l-1}}}}, \end{aligned} \tag{41}$$

where the conditional ambiguity estimates $\hat{N}^l_{j_l|j_1,\ldots,j_{l-1}}$ are determined by classical bootstrapping and, obviously depend on the path from j_1 to j_{l-1}. The standard deviations $\sigma^2_{\hat{N}_{l|1,\ldots,l-1}}$ are also known from bootstrapping and do only depend on the levels but not on the individual path. Eq. (41) provides a lower and upper bound for the fixing of N^k at path number j_k:

$$\begin{aligned} u_{\check{N}^k_{j_k}} &= \hat{N}_{j_k|j_1,\ldots,j_{k-1}} - \sigma_{\hat{N}_{j_k|j_1,\ldots,j_{k-1}}} \\ &\quad \cdot \sqrt{\chi^2 - \sum_{l=1}^{k-1} \frac{\left(\check{N}^l_{j_l} - \hat{N}^l_{j_l|j_1,\ldots,j_{l-1}}\right)^2}{\sigma^2_{\hat{N}_{l|1,\ldots,l-1}}}} \\ o_{\check{N}^k_{j_k}} &= \hat{N}_{j_k|j_1,\ldots,j_{k-1}} + \sigma_{\hat{N}_{j_k|j_1,\ldots,j_{k-1}}} \\ &\quad \cdot \sqrt{\chi^2 - \sum_{l=1}^{k-1} \frac{\left(\check{N}^l_{j_l} - \hat{N}^l_{j_l|j_1,\ldots,j_{l-1}}\right)^2}{\sigma^2_{\hat{N}_{l|1,\ldots,l-1}}}}, \end{aligned} \tag{42}$$

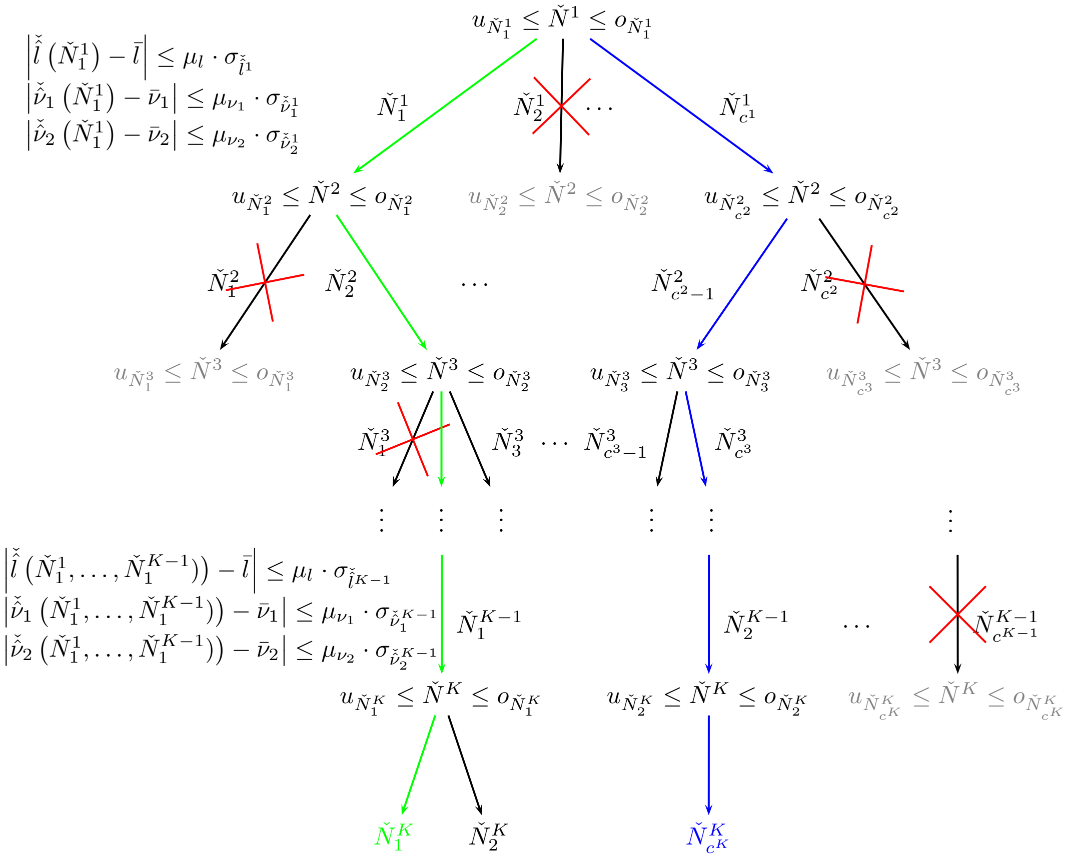

Fig. 7 Search tree: Constraints on the baseline length and orientation are checked at each path node to reduce the final number of branches. The tightness of the bounds and, thus, the efficiency of the search, is determined by the prefactors μ_l, μ_{ν_1} and μ_{ν_2}.

where the dependency on the previous path numbers $j_1, \ldots, j_{k-1}$ has been omitted to simplify notation. The tree is constructed sequentially with (42) and the total number of paths c^K is reduced by some constraints on the baseline estimate. The latter one is given for path number j_k by

$$\begin{bmatrix} \check{\hat{\boldsymbol{\xi}}}_{j_1,\ldots,j_k} \\ \check{\hat{\boldsymbol{N}}}_{j_1,\ldots,j_k} \end{bmatrix} = \left(\left[\boldsymbol{H} \;\; \boldsymbol{P}^k \boldsymbol{A}\right]^T \boldsymbol{\Sigma}^{-1} \left[\boldsymbol{H} \;\; \boldsymbol{P}^k \boldsymbol{A}\right]\right)^{-1} \left[\boldsymbol{H} \;\; \boldsymbol{P}^k \boldsymbol{A}\right]^T \boldsymbol{\Sigma}^{-1} \left(\boldsymbol{\Psi} - \bar{\boldsymbol{P}}^k \boldsymbol{A} \begin{bmatrix} \check{N}_{j_1} \\ \vdots \\ \check{N}_{j_k} \end{bmatrix}\right), \tag{43}$$

where the selection matrices $\boldsymbol{P}^k$ and $\bar{\boldsymbol{P}}^k$ are defined as

$$\begin{aligned} \boldsymbol{P}^k &= \begin{bmatrix} \boldsymbol{1}^{k \times k} \\ \boldsymbol{0}^{K-k \times k} \end{bmatrix} \\ \bar{\boldsymbol{P}}^k &= \begin{bmatrix} \boldsymbol{0}^{k \times K-k} \\ \boldsymbol{1}^{K-k \times K-k} \end{bmatrix}. \end{aligned} \tag{44}$$

The notation $(\check{\hat{\cdot}})$ has been introduced to denote partial fixing. The spherical baseline parameters can be easily obtained from the cartesian estimates:

$$\begin{aligned} \check{\hat{l}}\left(\check{N}_{j_1}^1, \ldots, \check{N}_{j_k}^k\right) &= \sqrt{\check{\hat{\xi}}_{x_{j_1,\ldots,j_k}}^2 + \check{\hat{\xi}}_{y_{j_1,\ldots,j_k}}^2 + \check{\hat{\xi}}_{z_{j_1,\ldots,j_k}}^2} \\ \check{\hat{\nu}}_1\left(\check{N}_{j_1}^1, \ldots, \check{N}_{j_k}^k\right) &= \arctan\left(\frac{\check{\hat{\xi}}_{z_{j_1,\ldots,j_k}}}{\sqrt{\check{\hat{\xi}}_{x_{j_1,\ldots,j_k}}^2 + \check{\hat{\xi}}_{y_{j_1,\ldots,j_k}}^2}}\right) \\ \check{\hat{\nu}}_2\left(\check{N}_{j_1}^1, \ldots, \check{N}_{j_k}^k\right) &= \arctan\left(\frac{\check{\hat{\xi}}_{y_{j_1,\ldots,j_k}}}{\check{\hat{\xi}}_{x_{j_1,\ldots,j_k}}}\right). \end{aligned} \tag{45}$$

The uncertainty of these parameters can be derived from the covariance matrix

$$\begin{aligned} \boldsymbol{\Sigma}_{\begin{bmatrix} \check{\hat{\boldsymbol{\xi}}} \\ \check{\hat{\boldsymbol{N}}} \end{bmatrix}} &= \begin{bmatrix} \boldsymbol{\Sigma}_{\check{\hat{\boldsymbol{\xi}}}}^k & \boldsymbol{\Sigma}_{\check{\hat{\boldsymbol{\xi}}}\check{\hat{\boldsymbol{N}}}} \\ \boldsymbol{\Sigma}_{\check{\hat{\boldsymbol{N}}}\check{\hat{\boldsymbol{\xi}}}} & \boldsymbol{\Sigma}_{\check{\hat{\boldsymbol{N}}}} \end{bmatrix} \\ &= \left(\left[\boldsymbol{H} \;\; \boldsymbol{P}^k \boldsymbol{A}\right]^T \boldsymbol{\Sigma}^{-1} \left[\boldsymbol{H} \;\; \boldsymbol{P}^k \boldsymbol{A}\right]\right)^{-1} \end{aligned} \tag{46}$$

which leads to

$$\sigma_{\check{\hat{l}}^k} = \sqrt{\operatorname{trace}\left(\boldsymbol{\Sigma}_{\check{\hat{\xi}}^k}\right)}. \tag{47}$$

The angle estimates $\check{\hat{\nu}}_1^k$ and $\check{\hat{\nu}}_2^k$ are not Gaussian distributed. Consequently, the standard deviations have to be determined by Monte-Carlo simulations from (45). The results could be stored in a look-up table for realtime applications.

Eq. (45) to (47) are the basis for the constraints on the baseline length and orientation given by

$$|\check{\hat{l}}\left(\check{N}_{j_1}^1, \ldots, \check{N}_{j_K}^K\right) - \bar{l}| \leq \mu_l \cdot \sigma_{\check{\hat{l}}^k} \tag{48}$$

and

$$\begin{aligned} |\check{\hat{\nu}}_1\left(\check{N}_{j_1}^1, \ldots, \check{N}_{j_K}^K\right) - \bar{\nu}_1| &\leq \mu_{\nu_1} \cdot \sigma_{\check{\hat{\nu}}_1^k} \\ |\check{\hat{\nu}}_2\left(\check{N}_{j_1}^1, \ldots, \check{N}_{j_K}^K\right) - \bar{\nu}_2| &\leq \mu_{\nu_2} \cdot \sigma_{\check{\hat{\nu}}_2^k}. \end{aligned} \tag{49}$$

The prefactors μ_l, μ_{ν_1} and μ_{ν_2} were introduced to control the tightness of the bounds and are constant over all levels. On the contrary, the standard deviations $\sigma_{\check{\hat{l}}^k}$, $\sigma_{\check{\hat{\nu}}_1^k}$ and $\sigma_{\check{\hat{\nu}}_2^k}$ reduce with increasing levels due to a larger number of fixed integer ambiguities.

Fig. 8 shows the number of paths as a function of prefactor μ_l for each level k. The benefit of tightening the constraint increases with the level k, i.e. the number of paths is reduced by only one order of magnitude for the first level but by three orders of magnitude at the last level. For $\mu_l \rightarrow \infty$, the number of paths converges to the number of paths of unconstrained ambiguity resolution. The simulation result refers to the estimation of the E1-E5 Galileo widelane ambiguities with wavelength of 78 cm for a geometry with 8 visible satellites and measurements from 5 epochs.

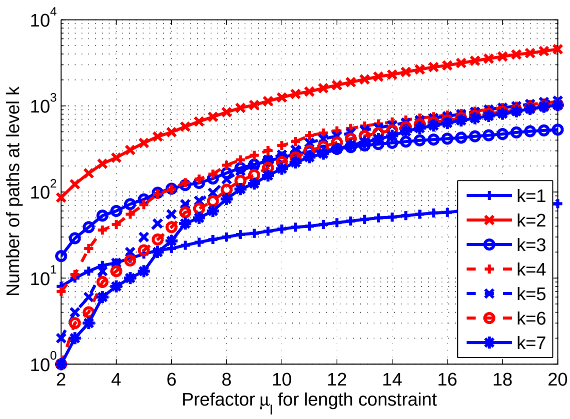

Fig. 8 Benefit of length constraint for integer search: The constraint reduces the number of paths by several orders of magnitude.

MULTI-FREQUENCY LINEAR COMBINATIONS

The reliability of carrier phase positioning can be further improved if a multi-frequency linear combination of ambiguities is resolved instead of the individual carrier phase ambiguities. This can be explained by the increase in the combination wavelength, which improves the conditioning of the equation system and, thereby, improves the accuracy of the float solution.

In [5]-[7], Henkel et al. optimized a class of multi-frequency linear combinations that include both code and carrier phase measurements with phase coefficients α_m and code coefficients β_m, i.e.

$$\lambda \phi^k = \sum_{m=1}^{M} \left(\alpha_m \lambda_m \phi_m^k + \beta_m \rho_m^k\right), \tag{50}$$

where $m = \{1, \ldots, M\}$ denotes the frequency index. The code and carrier phase measurements can be assumed statistically independent, such that the standard deviation of the combination noise is given by

$$\sigma = \sqrt{\sum_{m=1}^{M} \left(\alpha_m^2 \sigma_{\phi_m}^2 + \beta_m^2 \sigma_{\rho_m}^2\right)} \tag{51}$$

which depends on the code and phase noise variances. In this paper, the code noise standard deviations are set to the Cramer Rao lower bound. It is given in Tab. 1 for the GPS signals on L1, L2 and L5 at a carrier to noise power ratio of 45 dB-Hz.

Tab. 1 Cramer Rao bounds for GPS signals on L1, L2 and L5 at $C/N_0 = 45\text{dB-Hz}$

	Signal	BW [MHz]	CRB [cm]
L1-I	BPSK(1), C/A	$2 \cdot 1.023$	78.29
L1-I	BPSK(1), C/A	$20 \cdot 1.023$	25.92
L1-C	MBOC, OS	$20 \cdot 1.023$	11.13
L2-C	BPSK(1), OS	$20 \cdot 1.023$	25.92
L5-I L5-Q	BPSK(10), OS	$20 \cdot 1.023$	7.83

The linear combination shall scale the geometry term by a certain predefined factor h_1, i.e.

$$\sum_{m=1}^{M} (\alpha_m + \beta_m) \stackrel{!}{=} h_1, \tag{52}$$

where $h_1 = 0$ corresponds to a geometry-free and $h_1 = 1$ to a geometry-preserving combination. Similarly, the combined first order ionospheric delay shall be scaled by a predefined value h_2, i.e.

$$\sum_{m=1}^{M} (\alpha_m - \beta_m) q_{1m}^2 \stackrel{!}{=} h_2, \tag{53}$$

where the minus sign arises from the code carrier divergence. Moreover, the linear combination of ambiguities shall correspond to a single wavelength times a single integer ambiguity:

$$\sum_{m=1}^{M} (\alpha_m \lambda_m N_m) \stackrel{!}{=} \lambda N. \tag{54}$$

Tab. 2 Triple-frequency code carrier widelane combinations of maximum discrimination for $\sigma_\phi = 1\mathrm{mm}$ and $\sigma_{\rho_m} = \mathrm{CRB}_m$

h_1	h_2	L1		L2		L5		λ	σ	D
1	0	j_1	1	j_2	-5	j_3	4			
		α_1	18.5659	α_2	-72.3348	α_3	55.4567	3.533 m	10.3 cm	17.17
		β_1	-0.1394	β_2	-0.0424	β_3	-0.5060			
1	-0.1	j_1	1	j_2	-5	j_3	4			
		α_1	17.3827	α_2	-67.7249	α_3	51.9224	3.308 m	9.5 cm	17.46
		β_1	-0.1132	β_2	-0.0359	β_3	-0.4311			
0	-1	j_1	-1	j_2	5	j_3	-4			
		α_1	-12.5565	α_2	48.9213	α_3	-37.5063	2.389 m	9.5 cm	12.60
		β_1	0.3557	β_2	0.0657	β_3	0.7201			
0	0	j_1	0	j_2	-1	j_3	1			
		α_1	0	α_2	-4.0948	α_3	3.9242	1 m	1.3 cm	38.05
		β_1	0.0140	β_2	0.0113	β_3	0.1453			

Eq. (54) is equivalent to

$$N = \sum_{m=1}^{M} \underbrace{\frac{\alpha_m \lambda_m}{\lambda}}_{=j_m \overset{!}{\in} \mathbb{Z}} N_m. \tag{55}$$

Finally, the remaining degrees of freedom shall be used to maximize the ambiguity discrimination which was introduced in [5] as the ratio between the combination wavelength and the doubled standard deviation of the combination noise, i.e.

$$D = \frac{\lambda}{2\sigma}. \tag{56}$$

The ambiguity discrimination of (56) shall be maximized over λ and over all j_m and β_m, i.e.

$$\max_{j_1,\ldots,j_M,\lambda,\beta_1,\ldots,\beta_M} D, \tag{57}$$

which includes a numerical search and an analytical computation as described in details in [7]. The result of this optimization was derived for Galileo by Henkel and Günther in [5]-[7]. For GPS with its new signals, it is given in Tab. 2.

TEST SET-UP

In this section, the integer ambiguity resolution shall be verified with real measurements from two PolaRx3G Galileo receivers of Septentrio. Fig. 9 shows the measurement equipment. The two receivers were connected to two NavX multi-frequency Galileo signal generators of IFEN GmbH, which generate high frequency signals. The transmit power was set such that the average carrier to noise power ratio was 48 dB-Hz. The Galileo receivers continuously tracked the E1 and E5a signals over 30 minutes. The baseline length was fixed to 30 m.

Fig. 10 and 11 show that both the range residuals and the widelane float ambiguity estimates are unbiased. The noise in the float ambiguity estimates is significantly lower than one cycle, which indicates an extremely reliable integer ambiguity resolution. The range residuals are Gaussian distributed and refer to the fixed ambiguity solution. Their standard deviations vary around 1 cm, which can be explained from the 1 mm phase noise by its amplification due to double differencing (factor 2), widelaning (factor 4.1) and the dilution of precision.

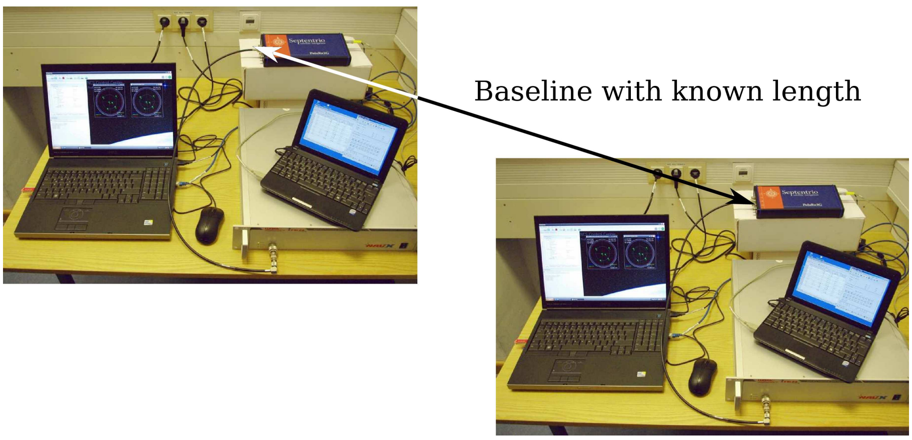

Fig. 9 Measurement equipment for constrained integer ambiguity resolution: Two PolaRx3G Galileo receivers of Septentrio are connected to two high frequency signal generators NavX of IFEN GmbH.

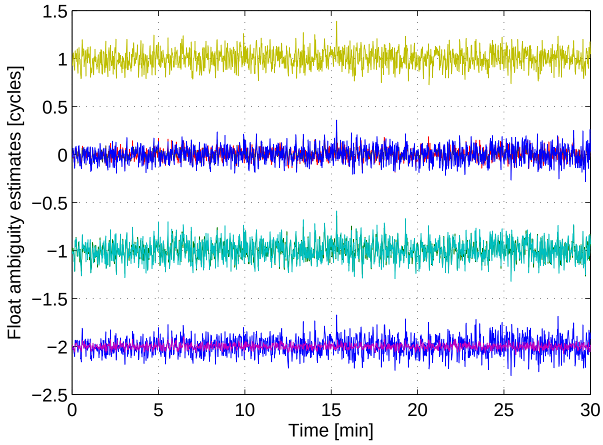

Fig. 10 Float estimates of the Galileo E1-E5a widelane ambiguities on a single epoch basis: The estimates are unbiased and the noise is significantly lower than one cycle.

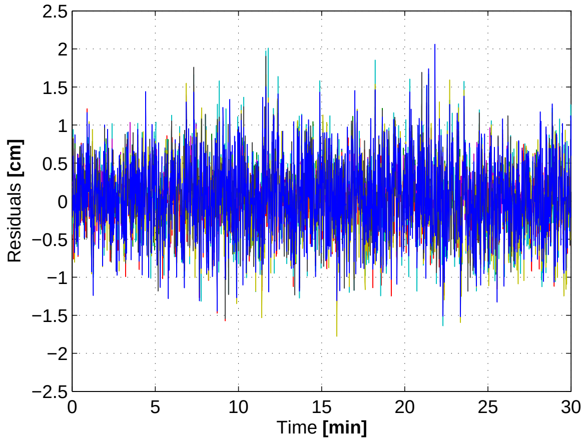

Fig. 11 Range residuals after widelane integer ambiguity resolution: The residuals of all widelane combinations are nearly unbiased and the noise level can be derived from the measurement noise and its amplification by double differencing, by the widelane combination and by the dilution of precision.

CONCLUSION

In this paper, a maximum a posteriori probability estimator was derived for the estimation of the baseline with both tight and soft constraints on the baseline length and orientation. This a priori information can be provided either as a Gaussian distribution or as a uniform distribution. The estimation includes a sequential construction of a search tree and an iterative solution with the Newton algorithm. The proposed algorithm has two advantages over unconstrained fixings: first, it reduces the number of paths in the search tree by several orders of magnitude. Secondly, the probability of wrong fixing is reduced but also the robustness over errors in the a priori information is substantially increased. The algorithm can be applied to multi-frequency combinations that increase the wavelength and, thereby, further improve the reliability of integer ambiguity resolution. The suggested algorithm can be used for any application where a precise and reliable relative position estimate is required and some a priori knowledge on the baseline length and/ or orientation is available.

ACKNOWLEDGEMENTS

The first author would like to thank the Institute of Navigation (ION) and the ESA Business Incubation Center (BIC) for the financial support of this trip. The second author would like to thank the German Federal Ministry of Economic Affairs and Technology (BMWi) and the German Aerospace Center (DLR) for a financial grant (FKZ: 50NA0911) to the project ”Multi-frequency ionospheric monitoring and ephemeris verification with Galileo” (MIMGAL) which supported this work.

REFERENCES

[1] P. Teunissen, The least-squares ambiguity decorrelation adjustment: a method for fast GPS ambiguity estimation, *J. of Geodesy*, vol. 70, pp. 65-82, 1995.

[2] R. Mönikes, J. Wendel and G. Trommer, A modified LAMBDA method for ambiguity resolution in the presence of position domain constraints, *Proc. of ION GPS*, pp. 81-87, 2005.

[3] P. Teunissen, The LAMBDA method for the GNSS compass, *Art. Satellites*, vol. 41, nr. 3, pp. 89-103, 2006.

[4] P. Teunissen, Integer least-squares theory for the GNSS compass, *J. of Geodesy*, vol. 84, pp. 433-447, 2010.

[5] P. Henkel and C. Günther, Joint L-/C-Band Code and Carrier Phase Linear Combinations for Galileo, *Int. J. of Nav. and Obs.*, Article ID 651437, 8 pp., 2008.

[6] P. Henkel, Bootstrapping with Multi-Frequency Mixed Code Carrier Linear Combinations and Partial Integer Decorrelation in the Presence of Biases, *Proc. of Int. Assoc. of Geod. Scient. Ass.*, Buenos Aires, Argentina, 2009.

[7] P. Henkel and C. Günther, Reliable Carrier Phase Positioning with Multi-Frequency Code Carrier Linear Combinations, *Proc. of 23rd ION Intern. Techn. Meet.* (ION-GNSS), Portland, USA, 2010.

[8] P. Jurkowski, Baseline constrained ambiguity resolution with multiple frequencies, *Bachelor thesis*, Technische Universität München, 49 pp., 2010.